Research Article

Journal of PeptideScience

Received: 18 May 2009 Revised: 28 May 2009 Accepted: 1 June 2009 Published online in Wiley Interscience: 13 July 2009

(www.interscience.com) DOI 10.1002/psc.1156

Design of potent 9-mer antimicrobial peptide analogs of protaetiamycine and investigation of mechanism of antimicrobial action‡

**Soyoung Shin,[a] Jin-Kyoung Kim,[a] Jee-Young Lee,[a] Ki-Woong Jung,[a] Jae-Sam Hwang,[b] Juneyoung Lee,[c] Dong Gun Lee,[c] Iksoo Kim,[d] Song Yub Shin[e] and Yangmee Kim[a]*

Protaetiamycine is an insect defensin, a naturally occurring 43-amino-acid-residue antimicrobial peptide derived from the larvae of the beetle *Protaetia brevitarsis*. In a previous work that aimed at developing short antibiotic peptides, we designed 9-mer peptide analogs of protaetiamycine. Among them, RLWLAIGRG-NH_2 showed good antifungal activity against *Candida albicans*. In this study, we designed four 9-mer peptide analogs based on the sequence of RLWLAIGRG-NH_2, in which Gly or Ile was substituted with Arg, Lys, or Trp to optimize the balance between the hydrophobicity and cationicity of the peptides and to increase bacterial cell selectivity. We measured their toxicity to bacteria and mammalian cells as well as their ability to permeabilize model phospholipid membranes. Substitution of Arg for Gly9 at the *C*-terminus (9Pbw1) resulted in two- to fourfold improvement in antibacterial activity. Further substitution of Gly7 with Lys (9Pbw2 and 9Pbw4) caused four- to eightfold improvement in the antibacterial activity without increase in cytotoxicity, while substitution of Gly7 with Trp (9Pbw3) increased cytotoxicity as well as antibacterial activity. The peptides 9Pbw2 and 9Pbw4 with the highest bacterial cell selectivity were not effective in depolarizing the membrane of *Staphylococcus aureus* cytoplasmic membranes and showed almost no leakage of a fluorescent dye entrapped within the vesicles. Gel-retardation experiments indicated that 9Pbw2 and 9Pbw4 inhibited the migration of DNA at concentrations >20 μM. Three positively charged residues at the *C*-terminus in 9Pbw2 and 9Pbw4 may facilitate effective penetration into the negatively charged phospholipid membrane of bacteria. The results obtained in this study suggest that the bactericidal action of our potent antibacterial peptides, namely 9Pbw2 and 9Pbw4, may be attributed to the inhibition of the functions of intracellular components after penetration of the bacterial cell membrane.

Keywords: protaetiamycine analogs; antimicrobial peptide; bacterial cell selectivity; intracellular mechanism

Introduction

Antimicrobial peptides are important components of the innate immune systems in all living organisms [1–4]. Many of these peptides rapidly kill invading pathogens by causing membrane permeabilization although this may not be their sole mode of action [2–6]. Since these peptides have a mechanism of action that differs from that of other therapeutic antibiotics, the former might constitute a class of attractive new drugs against microorganisms resistant to currently available antibiotics. The innate immune systems of invertebrates – of insects in particular – have revealed the importance of antimicrobial peptides for their defense. Insects are extremely resistant to bacterial infections [7]. A majority of such defensive peptides in insects are produced in either their fat body or hemocytes and then released into their hemolymph [8,9]. These peptides are known to play important roles in humoral defense reactions [10–14]. Thus far, more than 200 antibacterial peptides have been identified in insects. Most antimicrobial peptides from insects can be divided into three categories [15]. The largest category consists of peptides with intramolecular cystine disulfide bonds forming hairpin-like β-sheets or α-helical/β-sheet mixed structures. The second group has amphipathic α-helical structures, and the third group comprises proline-rich or glycine-rich peptides [15,16].

* *Correspondence to: Yangmee Kim, Department of Bioscience and Biotechnology, Konkuk University, 1 Hwayang-dong, Kwangjin-gu, Seoul 143-701, Korea. E-mail: ymkim@konkuk.ac.kr*

a *Department of Bioscience and Biotechnology, Konkuk University, Seoul 143-701, Korea*

b *Department of Agricultural Biology, National Institute of Agricultural Science and Technology, RDA, Suwon 441-100, Korea*

c *School of Life Sciences and Biotechnology, College of Natural Sciences, Kyungpook National University Daegu 702-701, Korea*

d *College of Agriculture and Life Sciences, Chonnam National University, Gwangju 500-757, Korea*

e *Research Center for Proteineous Materials and Department of Cellular and Molecular Medicine, School of Medicine, Chosun University, Gwangju 501-759, Korea*

‡ *Special issue devoted to contributions presented at the 1st Italy-Korea Symposium on Antimicrobial Peptides, 24–25 July 2008.*

Abbreviations used: *CD, circular dichroism; CH, cholesterol; diSC_3-5,3,3′-dipropylthiadicarbocyanine iodide; DMEM, Dulbecco's modified eagle's medium; DPC, dodecylphosphocholine; EYPC, egg yolk L-α-phosphatidylcholine; EYPG, egg yolk L-α-phosphatidylglycerol; FBS, fetal bovine serum; Fmoc, 9-fluorenylmethoxycarbonyl; h-RBCs, human red blood cells; LUV, large unilamellar vesicle; MHC, minimal hemolysis concentration; MIC, minimum inhibitory concentration; MTT, (3-(4,5-dimethylthiazol-2-yl)-2,5-diphenyltetrazolium bromide; PBS, phosphate buffered saline; SUV, small unilamellar vesicle; TFA, trifluoroacetic acid; TFE, 2,2,2-trifluoroethanol.*

In insects, the defensins comprise a large family of cationic cysteine-rich antimicrobial peptides; they are active against Gram-positive bacteria and filamentous fungi [17,18]. These cysteine-rich peptides display multifunctional properties with implications as potential therapeutic agents. We have previously identified a novel insect defensin from the larvae of a beetle, *Protaetia brevitarsis*, and named it as protaetiamycine [1]. In order to develop therapeutic peptide antibiotics, a 12-mer peptide segment from Ala19 to Gly30 in protaetiamycine (ACAAHCLAIGRG-NH_2) and its 9-mer derivatives, based on the sequence of protaetiamycin from Ala22 to Gly30, were synthesized. Among the six analogs, ALWLAIGRG-NH_2 (namely 9Pbw0) exhibited strong antifungal activity as compared with cecropin B [1].

Since a short antimicrobial peptide with bacterial cell selectivity would be an attractive candidate as a therapeutic agent, we designed four 9-mer analogs on the basis of the sequence of 9Pbw0. We measured their toxicities toward bacteria and mammalian cells, as well as their abilities to permeate model phospholipid membranes. In this study, we developed potent 9-mer peptide antibiotics without cytotoxicity and investigated their modes of action.

Experimental Procedures

Peptide Synthesis

All peptides specified in Table 1 were prepared by solid-phase synthesis using Fmoc chemistry. Peptides were purified by reversed-phase preparative high-performance liquid chromatography on a C_{18} column (20 × 250 mm; Shim-pack) using a gradient of 20–50% acetonitrile in H_2O with 0.1% TFA delivered over 30 min. Analytical high-performance liquid chromatography with an octadecylsilica (ODS) column (4.6 × 250 mm; Shim-pack) revealed that purified peptides were more than 95% homogeneous (data not shown). The peptides also had the correct atomic masses as determined by matrix-assisted laser desorption/ionization time-of-flight mass spectrometry (Table 1).

Antibacterial Activity

Escherichia coli (KCTC 1682), *Salmonella typhimurium* (KCTC 1926), *Pseudomonas aeruginosa* (KCTC 1637), *Bacillus subtilis* (KCTC 3068), *Staphylococcus epidermidis* (KCTC 1917), and *Staphylococcus aureus* (KCTC 1621) were purchased from the Korean Collection for Type Cultures (KCTC), Taejon, Korea. The clinical isolates of methicillin-resistant *S. aureus* (MRSA) (CCARM 3089, CCARM 3090, CCARM 3108, CCARM 3114 and CCARM 3126), multidrug-resistant *S. typhimurium* (MDRST) (CCARM 8003, CCARM 8007 and CCARM 8009), and multidrug-resistant *E. coli* (MDREC) (CCARM 1229 and CCARM 1238) were supplied from the Culture Collection of Antibiotic-resistant Microbes (CCARM) at Seoul Women's University in Korea. MIC test of peptides against bacteria was performed by broth microdilution method. The bacteria were grown to the mid-log phase in a medium (g/l) (10 bactotryptone/5 yeast extract/10 NaCl, pH 7.0). The peptides were filtrated through a 0.22 μm filter and stepwise diluted in a medium of 1% bactopeptone. The tested organism [final bacterial suspension: 2×10^6 colony-forming units (CFU)/ml], suspended in growth medium (100 μl), was mixed with 100 μl of the twofold-diluted serial solution of each peptide in a 96-well plate with three replicates for each test sample. The plates were incubated at 37 °C for 20 h. The MIC value was defined as the lowest concentration of antibiotic giving a complete inhibition of visible growth in comparison to an antibiotic-free control well. The experiments were replicated at least three times to verify the methodology reproducibility when using the above-mentioned conditions.

Hemolytic Activity

Hemolytic activity of the peptides was tested against h-RBC. Fresh h-RBCs were washed three times with PBS (PBS; 35 mM phosphate buffer containing 150 mM NaCl, pH 7.4) by centrifugation for 10 min at 1000 *g* and resuspended in PBS. The peptide solutions were then added to 50 μl of h-RBC in PBS to give a final volume of 100 μl and a final erythrocyte concentration of 4%, v/v. The resulting suspension was incubated with agitation for 1 h at 37 °C. The samples were centrifuged at 1000 *g* for 5 min. Release of hemoglobin was monitored by measuring the absorbance of the supernatant at 405 nm. Controls for no hemolysis (blank) and 100% hemolysis consisted of h-RBCs suspended in PBS and 0.1% Triton-X 100, respectively. The percent hemolysis was calculated using the following equation:

$$\text{Hemolysis (\%)} = [(OD_{405\ nm}\ \text{sample} - OD_{405\ nm}\ \text{zero lysis})/(OD_{405\ nm}\ 100\%\ \text{lysis} - OD_{405\ nm}\ \text{zero lysis})] \times 100 \quad (1)$$

Cytotoxicity

The human keratinocyte HaCaT cells (Heidelberg, Germany) were cultured at 37 °C in a 5% CO_2 atmosphere using DMEM supplemented with 10% heat-inactivated FBS and antibiotics (100 U/ml penicillin, 100 ug/ml streptomycin). Cells were maintained in suspension or as monolayer cultures, and subcultured. The percentage of growth inhibition was evaluated using a 3-(4,5-dimethylthiazol-2-yl)-5(3-carboxymethonyphenol)-2-(4-sulfophenyl)-2H-tetrazolium (MTS) assay for the measurement of viable cells. A total of 1×10^4 cells/well was seeded onto a 96-well plate for 24 h, treated with various concentrations of the

Table 1. Amino acid sequences and properties of protaetiamycin 9-mer analogs

Peptide	Sequence	Molecular mass (Da)	Net charge	Hydrophilicity[a]	Retention time (min)
9Pbw0	RLWLAIGRG-NH_2	1040.97	+3	−0.37	19.6
9Pbw1	RLWLAIGRR-NH_2	1140.08	+4	−0.03	18.8
9Pbw2	RLWLAIKRR-NH_2	1211.16	+5	0.34	17.6
9Pbw3	RLWLAIWRR-NH_2	1269.19	+4	−0.41	21.2
9Pbw4	RLWLAWKRR-NH_2	1283.79	+5	0.12	18.5

[a] Hydrophilicity is the total hydrophilicity (sum of all residue hydrophilicity indices) divided by the number of residues according to the Hopp and Woods index [19].

tested peptides, and then incubated for an additional 24 h at 37 °C. Subsequently, 20 µl of MTS at a concentration of 5 mg/ml was added to each of the wells, and the cells were incubated for additional 3 h. Absorbance was then measured at a wavelength of 492 nm using an ELISA reader.

Calcein Leakage Assay

Calcein-entrapped LUVs composed of EYPC/EYPG (7 : 3, w/w) and EYPC/CH (10 : 1,w/w) were prepared by vortexing the dried lipid in dye buffer solution (70 mM calcein, 10 mM Tris, 150 mM NaCl, 0.1 mM EDTA, pH 7.4) [20]. The suspension was frozen-thawed in liquid nitrogen for ten cycles and extruded through polycarbonate filters (two stacked 100 nm pore size filters) by a LiposoFast extruder (Avestin, Canada). Untrapped calcein was removed by gel filtration on a Sephadex G-50 column. Usually lipid vesicles were diluted to approximately tenfold after passing through a Sephadex G-50 column. The eluted calcein-entrapped vesicles were diluted further to the desired final lipid concentration for the experiment. The leakage of calcein from the LUVs was monitored by measuring fluorescence intensity at an excitation wavelength of 490 nm and an emission wavelength of 520 nm on a model RF-5301PC spectrophotometer (Shimadzu, Kyoto, Japan). For determination of 100% dye-release, 10% Triton-X_{100} in Tris-buffer (20 µl) was added to dissolve the vesicles. The percentage of dye-leakage caused by the peptides was calculated as follows:

$$\text{Dye-leakage (\%)} = 100 \times (F - F_0)/(F_t - F_0) \quad (2)$$

where F is the fluorescence intensity shown by the peptides, and F_0 and F_t are fluorescence intensities without the peptides and with Triton X-100, respectively.

Tryptophan Fluorescence Blue Shift

SUVs composed of either EYPC or EYPG, which minimize differential light-scattering effects [21], were prepared by sonication [22]. All fluorescence measurements were performed in quartz cuvettes with a 1 cm path length. SUVs were added to a peptide solution (3 µM final concentration) in 10 mM Tris-buffer (pH 7.4), 0.1 mM EDTA, and 150 mM NaCl, and maintained at 25 °C with continuous stirring in a total volume of 3 ml. The lipid concentration was 600 µM. Fluorescence spectra were measured using a Shimadzu RF 5301 PC spectrofluorimeter at emission and excitation band passes of 5 nm. Tryptophan residues of each peptide were excited at 280 nm, and emission spectra were recorded in the range 300–400 nm.

Membrane Depolarization

The membrane depolarization activity of peptides was determined using intact *S. aureus* cells and the membrane potential-sensitive fluorescent dye, $diSC_3$-5 on the basis of the methods of Friedrich *et al*. [23]. *S. aureus*, grown at 37 °C with agitation to mid-log phase (OD600 = 0.4), was harvested by centrifugation. The cells were washed twice with buffer (20 mM glucose, 5 mM 4-(2-hydroxyethyl)-1-piperazineethanesulfonic acid (HEPES), pH 7.4) and resuspended to an OD600 of 0.05 in a similar buffer containing 0.1M KCl. Then, the cells were incubated with 20 nM $diSC_3$-5 until a stable reduction of fluorescence was achieved, indicating the incorporation of the dye into the bacterial membrane. Membrane depolarization was then monitored by observing the change in the intensity of fluorescence emission of the membrane potential-sensitive dye $diSC_3$-5 ($\lambda ex = 622$ nm, $\lambda em = 670$ nm) after the addition of peptides. Full dissipation of the membrane potential was obtained by adding gramicidin D (MP Biomedical, LLC), final concentration being 0.2 nM. The membrane potential-dissipating activity of the peptides is expressed as follows:

$$\text{\% Membrane depolarization} = 100 \times (F_p - F_0)/(F_g - F_0) \quad (3)$$

where F_0 is the fluorescence value after addition of the $diSC_3$-5 dye, F_p is the fluorescence value 5 min after addition of the peptides, and F_g the fluorescence signal after the addition of gramicidin D.

DNA-binding Assay

Gel-retardation experiments were performed by mixing 100 ng of the plasmid DNA (pBluescript II SK+) with increasing amounts of peptide in 20 µl of binding buffer (5% glycerol, 10 mM Tris-HCl at pH 8.0, 1 mM EDTA, 1 mM dithiothreitol, 20 mM KCl, and 50 µg/ml bovine serum albumin). The reaction mixtures were incubated at room temperature for 1 h. Subsequently, 4 µl of native loading buffer was added (10% Ficoll 400, 10 mM Tris-HCl at pH 7.5, 50 mM EDTA, 0.25% bromophenol blue, and 0.25% xylene cyanol), and a 20 µl aliquot was applied to a 1% agarose gel electrophoresis in 0.5× Tris borate-EDTA buffer (45 mM Tris-borate and 1 mM EDTA at pH 8.0) [24]. The plasmid DNA used in this experiment was purified by CsCl-gradient ultracentrifugation to select the closed circular form of the plasmid.

CD Analysis

CD experiments were performed using a J-810 spectropolarimeter (Jasco, Tokyo, Japan) with a 1-mm path length cell. The CD spectra of the peptides at 100 µM were recorded at 25 °C at 0.1-nm intervals from 190 to 250 nm. To investigate the conformational changes induced by membrane environments, TFE/water solution and 50 mM DPC micelles were added to the peptides. For each spectrum, the data from ten scans was averaged and smoothed using J-810. CD data are expressed as the mean residue ellipticity [θ] in deg·cm^2/dmol.

NMR Experiments

9Pbw2 and 9Pbw4 with the highest bacterial cell selectivities were dissolved at 1.0 mM in 0.45 ml of a 9 : 1 (v/v) H_2O/D_2O (pH 6.0) solution containing DPC micelles. Perdeuterated DPC was purchased from Cambridge Isotope Laboratories (Andover, MA). In order to investigate the conformational changes of peptides in the presence of DPC micelles, 1D ^{1}H NMR spectra of 9Pbw2 and 9Pbw4 were recorded for different concentrations of DPC For the assignment of the NMR spectra, phase-sensitive two-dimensional experiments, including double-quantum-filtered (DQF) COSY, TOCSY, and NOESY, were performed by time-proportional phase incrementation [25–28]. TOCSY experiments were performed using 50- and 80-ms MLEV-17 spin-lock mixing pulses. Mixing times of 150, 250, and 350 ms were used for NOESY experiments. Chemical shifts are expressed relative to the 4,4-dimethyl-4-silapentane-1-sulfonate signal at 0 ppm. All of the NMR spectra were recorded on a Bruker 400 MHz spectrometer at Konkuk University and a 600 MHz spectrometer at KBSI (Korea Basic Science Institute) in Ochang-eup, Cheongwon-gun, Chungbuk, Korea. NMR spectra were processed with NMRPipe [29] and visualized with Sparky [30].

Results and Discussion

Peptide Design

Saido-Sakanaka *et al*. [31] reported the synthesis and characterization of analogs designed on the basis of the insect peptide defensin – comprising 43 amino acids -extracted from the beetle *Allomyrina dichotoma*. They synthesized 12-mer (LCAAHCLAIGRR-NH_2: 19L-30R-NH_2) and 9-mer (AHCLAIGRR-NH_2: 22A-30R-NH_2) defensin segments, which show antimicrobial activity [31]. Furthermore, they synthesized two 9-mer derivatives, peptide A (RLYLRIGRR-NH_2) and peptide B (RLRLRIGRR-NH_2), by replacing Ala1 with Arg, His2 with Leu, and Cys3 with Tyr or Arg. Furthermore, a hydrophobic residue, Ala5, in the middle of the peptide, was substituted with a positively charged Arg in both peptides A and B. These peptides had a therapeutic effect on MRSA infections in mice and exhibited anti-inflammatory effects by inhibiting tumor necrosis factor-alpha (TNF-α) production [32,33]. Peptide A has a net charge of +5 and a hydrophilicity of 0.48, as calculated by the Hopp and Woods index [19]. Peptide B has a net charge of +6 and a hydrophilicity of 1.07. Therefore, these peptides are highly positively charged.

In our previous study, we have characterized a new insect defensin, protaetiamycine, extracted from the larvae of the beetle *P. brevitarsis* [1]. Protaetiamycine has 72% sequence homology with the defensin from the beetle *A. dichotoma*. We have designed a 9-mer peptide analog RLWLAIGRG-NH_2 (9Pbw0) from protaetiamycine [1]. However, 9Pbw0 has considerably lower antibacterial activity as compared to melittin. In order to design a more potent antibacterial peptide, we substituted Gly9 at the *C*-terminus with Arg (9Pbw1). To improve the antibacterial activity, we increased the cationicity by a further substitution of Gly7 with Lys (9Pbw2) or increased the hydrophobicity by further substitution of Gly7 with Trp (9Pbw3) as listed in Table 1. To enhance the antibacterial activity without increasing hydrophobicity, we substituted Ile6 with Trp and Gly7 with Lys (9Pbw4). We ensured that the residues from two to six in the middle of the sequence were hydrophobic and the residues at the *N*- and *C*-termini were cationic. Therefore, compared to the 9-mer analogs of the beetle *A. dichotoma,* our peptide analogs were designed to retain an amphipathic structure. The relative hydrophobicity of the peptides was determined by measuring their retention times in reverse-phase HPLC. Table 1 lists the sequences of the peptides, net charges, and hydrophilicities calculated by using the Hopp and Woods index [19]. The lower the hydrophilicity, the higher is the hydrophobicity. A peptide with a longer retention time has a higher hydrophobicity. Therefore, the relative hydrophobicity of the peptides increased in the following order: 9Pbw2 < 9Pbw4 < 9Pbw1 < 9Pbw0 < 9Pbw3, as listed in Table 1.

Antimicrobial Activity and Hemolytic Activity

The antimicrobial activities of the peptides were examined against a representative set of bacterial strains, including three Gram-negative species (*E. coli, S. typhimurium*, and *P. aeruginosa*) and three Gram-positive species (*B. subtilis, S. epidermidis*, and *S. aureus*), as listed in Table 2. All of the peptides demonstrated high antibacterial activities against standard strains. 9Pbw1 with Arg substitution for Gly9 in 9Pbw0 demonstrated a two- to fourfold improvement in the antibacterial activity over that of 9Pbw0. Other peptides with more Lys (9Pbw2 and 9Pbw4) or Trp (9Pbw3) had four- to eightfold improved antibacterial activity as compared to 9Pbw0. We introduced the geometric mean (GM) of the MIC values from all standard bacterial strains to determine an overall evaluation of the peptide antimicrobial activity against both Gram-positive and Gram-negative bacteria. The antimicrobial activity of the peptides increased in the following order: 9Pbw0 < 9Pbw1 < 9Pbw3 < 9Pbw2 = 9Pbw4.

Furthermore, the antimicrobial activities of the peptides were examined against ten antibiotic-resistant bacterial strains, as listed in Table 3. All peptides demonstrated high antibacterial activities against antibiotic-resistant bacterial strains. 9Pbw3 is the most active among all analogs against MRSA, while 9Pbw2 and 9Pbw4 are even more potent than melittin for MDRST and MDREC.

We checked the hemolytic activity of the peptides. The dose-response curves for the hemolytic activity of the peptides are shown in Figure 1. None of the peptides, with the exception of 9Pbw3, showed hemolytic activity even at 100 μM. 9Pbw3 with two Trp residues was highly cytotoxic and showed hemolytic activity over 40% at 100 μM. However, at their MIC, none of the peptides showed hemolytic activity.

Table 2 lists the MHC values against h-RBCs, the GM of the MIC value for all bacterial strains, and the therapeutic index (MHC/GM), which is the ratio of MHC to the average MIC. Thus, a high therapeutic index is an indication of the two preferred characteristics of the peptide: a high MHC (low hemolysis) and a low MIC (high antimicrobial activity). 9Pbw2 and 9Pbw4 showed

Table 2. Antimicrobial activities against standard bacterial strains and hemolytic activities of the peptides

	MIC[a] (μM)								
Peptide	*E. coli*	*P. aeruginosa*	*S. typhimurium*	*B. subtilis*	*S. epidermidis*	*S. aureus*	GM[b] (μM)	MHC[c] (μM)	Therapeutic index[d] (MHC/GM)
9Pbw0	8	>32	32	8	4	16	16.7	≥100	≥6
9Pbw1	4	16	16	4	2	4	7.7	≥100	≥13
9Pbw2	2	8	2	2	1	2	2.8	≥100	≥35
9Pbw3	2	16	8	2	1	2	5.2	25	4.8
9Pbw4	2	8	2	2	1	2	2.8	≥100	≥35
Melittin	1	2	2	2	1	2	1.7	0.20	0.1

[a] MIC values were determined in three independent experiments performed in triplicate with a standard deviation of 14.0%.
[b] The geometric mean (GM) of the MIC values from all six bacterial strains in this Table.
[c] The minimal peptide concentration that produces hemolysis. When no detectable hemolysis was observed at 100 μM, we used a value of 100 μM as MHC to calculate the therapeutic index.
[d] The ratio of the MHC (μM) over the geometric mean (GM) of the MIC (μM). Larger values indicate greater cell selectivity.

Journal of PeptideScience

Table 3. Antimicrobial activities of the peptides against antibiotic-resistant bacterial strains

	MIC(μM)									
	Antibiotic-resistant bacterial strains									
Peptides	*S. aureus 3089(R)*	*S. aureus 3090(R)*	*S. aureus 3108(R)*	*S. aureus 3114(R)*	*S. aureus 3126(R)*	*S. typhimu. 8003(R)*	*S. typhimu. 8007(R)*	*S. typhimu. 8009(R)*	*E. coli 1229(R)*	*E. coli 1238(R)*
9Pbw0	16	16	16	32	16	>32	>32	>32	16	8
9Pbw1	8	8	4	16	8	32	32	32	8	8
9Pbw2	4	4	4	8	8	4	8	4	4	4
9Pbw3	2	2	2	4	4	16	16	8	8	4
9Pbw4	4	4	4	8	4	4	8	4	4	4
Melittin	2	2	1	2	2	8	8	8	4	8

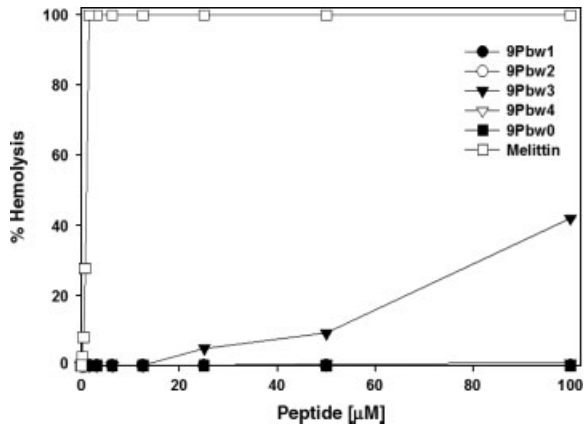

Figure 1. Dose-response of hemolytic activity of the peptides against h-RBCs.

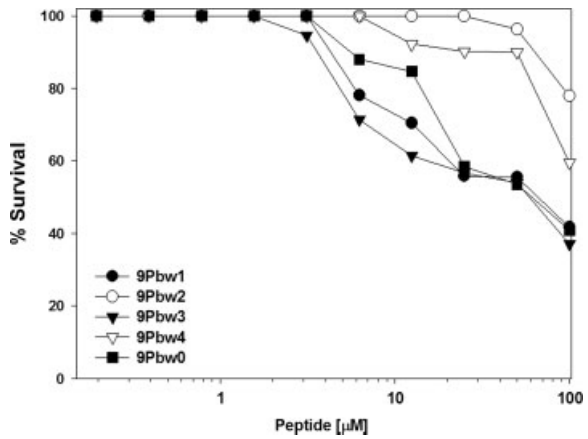

Figure 2. Dose-response of cytotoxic activity of the peptides against HaCaT cells.

high antibacterial activity without cytotoxicity, resulting in high bacterial cell selectivity and therapeutic index.

Cytotoxicity against Mammalian Cells

We next examined the cytotoxicity of the peptides against HaCaT cells. The effects on cell growth, which were assessed by measuring the mitochondrial conversion of MTT to a colored formazan product, are shown in Figure 2. 9Pbw0, 1, and 3 showed remarkable cytotoxicity against the HaCaT cells at 50 μM, while 9Pbw2 and 9Pbw4 showed a survival rate greater than 80% at 50 μM. These data imply that hydrophobicity (9Pbw0, 1, and 3 have longer retention times than 9Pbw2 and 9Pbw4) is an important factor for cytotoxicity. Moreover, 9Pbw2 and 9Pbw4 have +5 net charges, while other peptides have lower net positive charges. Cationicity is an integral component of antimicrobial peptide interactions with negatively charged phospholipid membranes of bacteria and other microorganisms. Hydrophobicity influences not only the antimicrobial activity but also the cytotoxicity of the peptide.

Tryptophan Fluorescence Blue Shift

The Trp residues in several types of antibacterial peptides such as melittin, mastoparan B, and IsCT have been reported to be critical for their antibacterial or hemolytic activities [34–36]. In order to investigate the interactions between the Trp residue and the phospholipid membrane, fluorescence emissions of Trp residues in our peptides were monitored in the Tris-HCl buffer (pH 7.4) or in the presence of vesicles composed of either zwitterionic phospholipids [EYPC/CH (10 : 1, w/w) SUVs] or negatively charged phospholipids [EYPC/EYPG (7 : 3, w/w) SUVs] (Table 4). Melittin, which is known to have not only high antibacterial activity but also high cytotoxicity, showed large blue shifts in both vesicles, implying that it is not cell selective. 9Pbw0, 9Pbw1, 9Pbw2, and 9Pbw4 exhibited considerably smaller blue shifts in the zwitterionic vesicles than in the negatively charged vesicles. This finding suggests that the Trp3 residue in these peptides does not penetrate deeply into the zwitterionic phospholipid vesicles, which mimic mammalian membranes, resulting in high bacterial cell selectivity. 9Pbw3 has two Trp residues at positions 3 and 7 while 9Pbw4 has Trp residues at positions 3 and 6. Therefore, 9Pbw3 has a longer hydrophobic stretch (from Leu2 to Trp7) than the other peptides. 9Pbw3 showed a considerably greater blue shift in the zwitterionic phospholipid vesicles as compared to 9Pbw4, implying that Trp7 in 9Pbw3 penetrates deeper into the zwitterionic phospholipid vesicle than Trp6 in 9Pbw4. This result agrees well with the lower hydrophilicity and longer retention time of 9Pbw3 than those of 9Pbw4 (Table 1). These data also correlate well with the high cytotoxicity of 9Pbw3. Further, 9Pbw2 has the highest hydrophilicity and the largest blue shift in negatively charged vesicles as compared to those of other peptides, suggesting that the positively charged Lys and the three Arg residues enhance the interactions with the negatively charged vesicles. The fluorescence blue shift data imply that Trp7 and hydrophobicity in 9Pbw3 may

Table 4. Tryptophan emission maximum of the peptides in Tris-HCl buffer (pH 7.4) or in the presence of EYPC/EYPG (7 : 3, w/w) liposomes and EYPC/CH (10 : 1, w/w) liposomes

Peptides	Sequences	Tris-buffer (pH 7.4)	EYPC/EYPG (7 : 3, w/w)	EYPC/CH (10 : 1, w/w)
9Pbw0	RLWLAIGRG-NH_2	349.2	344.6(−4.6)	349.6(0.4)
9Pbw1	RLWLAIGRR-NH_2	349.6	342.8(−6.8)	348.8 (−0.8)
9Pbw2	RLWLAIKRR-NH_2	350.0	336.0(−14.0)	349.4(−0.6)
9Pbw3	RLWLAIWRR-NH_2	350.6	340.2 (−10.4)	345.6 (−5)
9Pbw4	RLWLAWKRR-NH_2	349.4	341.6 (−7.8)	347.2 (−2.2)
Melittin	GIGAVLKVLTTGLPALISWIKRKREE-NH_2	348.8	331.4 (−17.4)	334.6(−14.2)

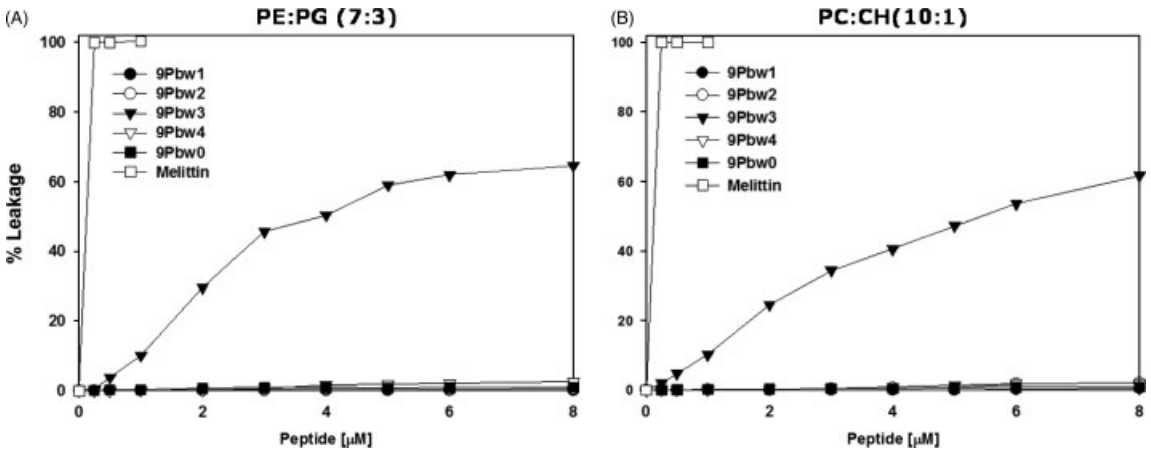

Figure 3. Dose-response curves of calcein leakage from (A) EYPC/EYPG (7 : 3, w/w) LUVs and (B) EYPC/CH LUVs (10 : 1, w/w) induced by the peptides. Calcein leakage was measured 2 min after adding the peptide. The lipid concentration used in the leakage experiments was 200 μM.

greatly influence the cytotoxicity of 9Pbw3 against mammalian cell membranes, while Trp3 and the positively charged residues in these peptides may play a considerable role in their antibacterial activity. Recently, it has been reported that peptide partition between the water and membrane phases can be investigated by Trp emission-shift data. Further investigation can be performed by measuring the changes in peptide fluorescence caused by titration of a peptide solution with phospholipid vesicles [37].

Peptide-induced Permeabilization of Lipid Vesicles

To investigate the membrane-permeabilizing ability of the peptides, we measured the release of the fluorescent marker calcein from liposomes of different compositions. We employed zwitterionic LUVs composed of 10 : 1(w/w) EYPC/CH, a phospholipid used to mimic the major components of the outer leaflet of human erythrocytes, and negatively charged LUVs composed of 7 : 3 (w/w) EYPC/EYPG to mimic bacterial cells. The percentage of calcein leakage 3 min after exposure to the peptide was used to assess its ability to permeate the membrane. Figure 3 shows the dose-response relationship of the peptide-induced calcein release. 9Pbw3 with Trp3 and Trp7 residues potently permeate both bacterial cell component membranes and zwitterionic vesicles. However, none of the other peptides permeate the negatively charged vesicles that mimic the bacterial cell component membranes and the zwitterionic vesicles. These results suggest that the antibacterial activity of these peptides may be not due to permeabilization of the bacterial cell membrane.

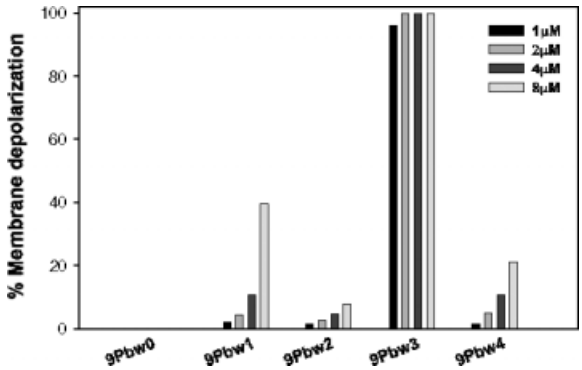

Figure 4. Dose-dependent dissipation of the transmembrane potential of *S. aureus* cells (OD600 = 0.05) by the peptides. The membrane potential-dissipating activity of the peptides is expressed as follows: % Membrane depolarization = $100 \times [(F_p - F_0)/(F_g - F_0)]$, where F_0 is the fluorescence value after addition of the $diSC_3$-5 dye, F_p is the fluorescence value 5 min after addition of the peptides, and F_g is the fluorescence signal after the addition of gramicidin D.

Dose-dependent Dissipation of the Transmembrane Potential of *S. aureus* Cells

We used dose-dependent dissipation of the transmembrane potential of intact *S. aureus* cells to further examine the ability of the peptides to permeate bacterial membranes. Peptide-induced membrane permeabilization induces a dissipation of the transmembrane potential that is monitored by an increase in fluorescence due to the release of the membrane potential-sensitive

Journal of PeptideScience

fluorescent dye $diSC_3$-5. Upon addition of the dye to a suspension of *S. aureus*, its fluorescence is strongly quenched as it deeply enters the membrane. Subsequent addition of peptides results in an increase in the $diSC_3$-5 fluorescence, reflecting the membrane depolarization. As shown in Figure 4, we found that 9Pbw3 can depolarize 100% of the cytoplasmic membrane of intact *S. aureus* at its MIC (2 μM) which is comparable to melittin activity, strongly suggesting that the bacterial cytoplasmic membrane is a major target of this peptide. In contrast, 9Pbw0, with weak antimicrobial activity, shows no depolarization and 9Pbw1 has 12% depolarization against *S. aureus* at its MIC (4 μM). 9Pbw2 and Pbw4 show less than 5% depolarization against *S. aureus* at their MIC (2 μM). These results suggest that the mode of the antibacterial activity of these peptides differ from that of 9Pbw3.

DNA-binding Activity

We next examined the DNA-binding properties of the 9Pbw2 and 9Pbw4 analogs with the highest therapeutic index in order to clarify their molecular mechanisms of action. We determined the DNA-binding affinities of the peptides by analyzing the electrophoretic mobility of the DNA bands at various ratios of peptides to DNA concentrations on an agarose gel (1%, w/v) following earlier protocols used for different AMPs [24]. 9Pbw2 and Pbw4 similarly inhibited the migration of DNA at concentrations >20 μM, as shown in Figure 5. Therefore, these peptides penetrated the cells without inducing any severe membrane permeabilization. In contrast to membrane-active peptides, these peptides might target nonmembrane intracellular components by inhibiting protein or DNA or RNA synthesis [38,39].

CD Measurements

We investigated the secondary structures of peptides in water and in membrane-like environments by analyzing their CD spectra. All peptides show unordered structures in aqueous solution, but they exhibit conformational changes in a 50% TFE/water solution and in DPC micelles (Figure 6). In general, interpretation of the CD spectra of these peptides is complicated by the presence of the Trp chromophoric side chain, preventing a detailed analysis of their secondary structures. Positive CD bands in the 220–230 nm region are mostly due to the Trp indole ring [40]. In TFE and DPC micelles the peptides show a positive trend at 190 nm and a negative maximum in the range 201–205 nm. These data imply that they may adopt a β-turn structure component [41,42]. Under these conditions, some peptides, in particular 9Pbw3, are characterized by double negative maxima at 205 and 220 nm, suggesting that they may be significantly folded in an α-helical structure under these conditions.

NMR Spectroscopy

Changes of chemical shifts and line broadenings in the 1D ^1H NMR spectra of 9Pbw2 and 9Pbw4 at 298 K in a 9:1 (v/v) H_2O/D_2O solution (pH 4.2) upon addition of DPC were investigated. We recorded sets of spectra for the peptides following their interaction with micelles at different concentrations of DPC. Figure 7 shows the NH region of the ^1H NMR spectra for 9Pbw2 and 9Pbw4. As illustrated in the spectra of 9Pbw2 (Figure 7A), addition of DPC resulted in the downfield shift of one indole proton of Trp3 in the 10–11 ppm region. Also, large chemical shift changes in the NH and the aromatic ring regions were seen. As 9Pbw4 has two Trp residues, the region from 10 to 11 ppm would be expected to exhibit two peaks. As shown in Figure 7B, addition of DPC to water caused large downfield shifts as well as the appearance of resolved resonances associated with the two indole NH protons of Trp3 and Trp6 in 9Pbw4. These changes imply that 9Pbw2 and 9Pbw4 have unordered structures in aqueous solution while they form more ordered structures in micellar environments which mimic the amphipathic environment of a phospholipid bilayer [43,44]. The addition of DPC induced line broadening and changes in chemical shifts up to 30 mM DPC. These spectral changes implied interactions between the peptides and the DPC micelles, resulting in more ordered structures for the peptides in the latter environment, confirming the conclusions extracted from the CD investigation (Figure 6).

We made sequence-specific resonance assignments of 9Pbw4 using mainly the DQF-COSY, TOCSY, and NOESY methods published by Wüthrich [45]. Resonances for Arg1 at the *N*-terminus were not observed and some cross peaks for Lys7, Arg8, and Arg9 were not resolved because of severe spectral overlap. Since 9Pbw2 and 9Pbw4 are small peptides (nine residues), not surprisingly there were not enough NOEs for an accurate structural calculation of peptides using NMR data.

Conclusion

In this research, we attempted to develop peptide antibiotics with selectivity for bacterial cells by synthesizing four 9-mer

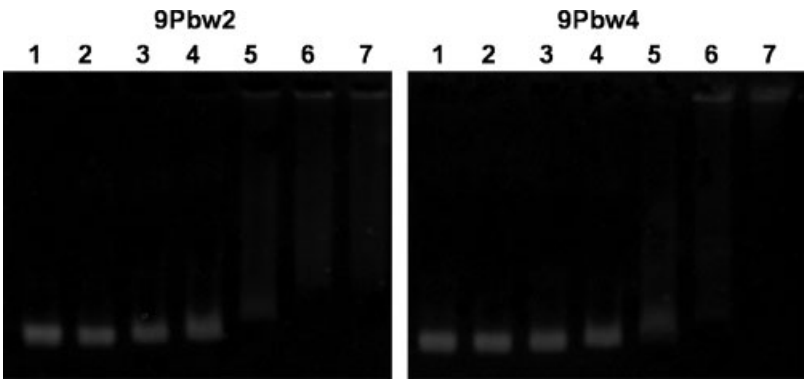

Figure 5. Gel-retardation assays of 9Pbw2 and 9Pbw4. Binding was assayed by measuring the inhibition of migration by plasmid DNA (100 ng; pBluescript II SK+). Lane 1, plasmid DNA alone; lane 2, 1 μM peptide; lane 3, 5 μM peptide; lane 4, 10 μM peptide; lane 5, 20 μM peptide; lane 6, 50 μM peptide; and lane7, 100 μM peptide. DNA and the peptides were co-incubated for 1 h at room temperature before electrophoresis on a 1.0% agarose gel.

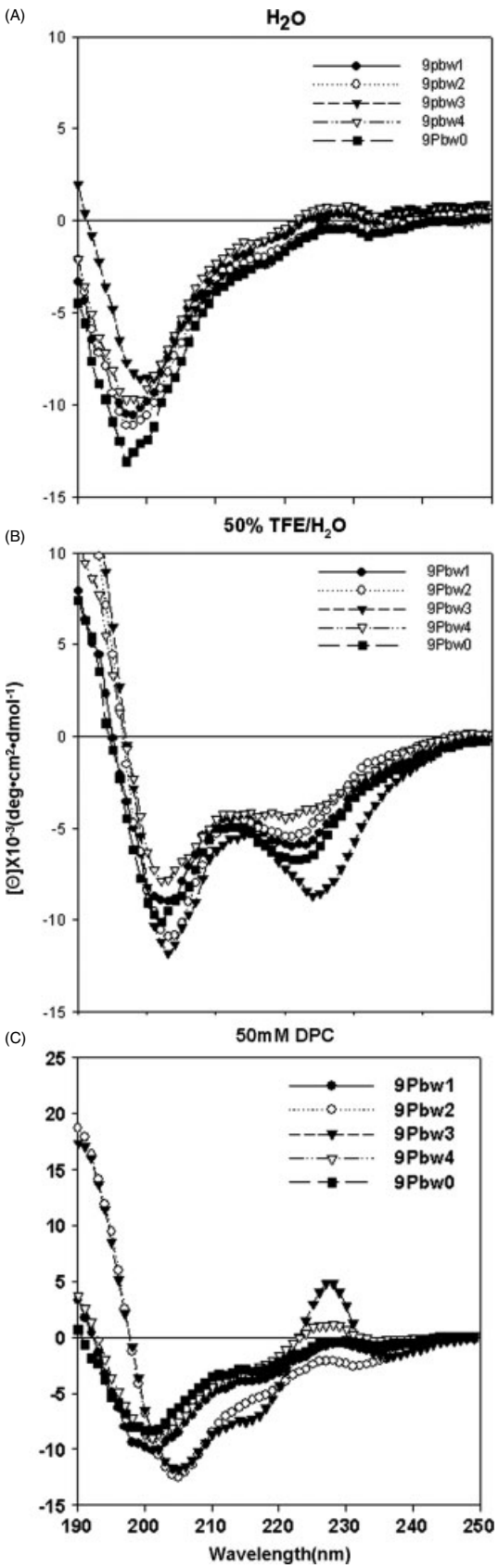

Figure 6. CD spectra of the peptides in (A) H_2O, (B) 50% TFE/water solution, and (C) 50 mM DPC micelles.

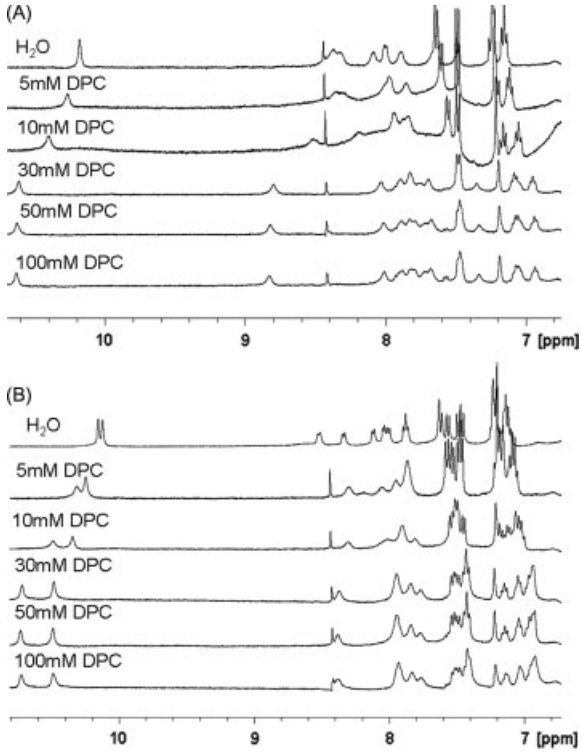

Figure 7. Changes of chemical shifts and line broadenings in the NH region of the ^{1}H NMR spectra at 298 K in 9 : 1 (v/v) H_2O/D_2O induced by DPC. Sets of 1D ^{1}H NMR spectra of a 1 mM solution of 9 Pbw2 (A) and 9Pbw4 (B) were recorded for different concentrations of DPC.

analogs of protaetiamycin. In order to develop antibiotic drugs with therapeutic potential, the peptide must be toxic toward bacterial cells but not significantly toxic to mammalian cells. Antimicrobial activity (Tables 2 and 3), hemolytic activity (Figure 1), and cytotoxicity (Figure 2) data indicated that 9Pbw3, with the highest hydrophobicity, is most cytotoxic to mammalian cells. Table 2 lists the therapeutic index, i.e. the ratio of MHC to the average MIC, for the peptides examined. 9Pbw2 and 9Pbw4 show high antibacterial activity without cytotoxicity, resulting in high bacterial cell selectivity (therapeutic index = 35). 9Pb2w and 9Pbw4 are even more potent than melittin for MDRST and MDREC as listed in Table 3. Therefore, we consider them as potent therapeutic agents.

The 9Pbw2 and 9Pbw4 peptides, which have the highest therapeutic index for the tested bacteria, are not effective at depolarizing the membrane potential of *S. aureus* cytoplasmic membrane and cause a very small amount of leakage of the fluorescent dye entrapped within negatively charged as well as neutral vesicles. These results suggest that the bactericidal action of these peptides is not due to the formation of transmembrane channels nor to the perturbation of the cell membrane. The results of the DNA-binding assay imply that, once in the cytoplasm, they may bind to intracellular components such as DNA and inhibit the activity of specific molecular targets essential to bacterial growth, thereby causing cell death. 9Pbw2 and 9Pbw4 have three positively charged residues at the *C*-terminus and one Arg at the *N*-terminus, while they have five hydrophobic residues in the middle portion. The CD and NMR spectra showed that these peptides, when bound to DPC micelles, have more ordered structures than those in aqueous solution. Three positively charged residues from position 6 to 9 at the *C*-terminus in 9Pbw2 and 9Pbw4

may be important for the primary binding to the negatively charged phospholipid head groups in bacterial cell membranes and critical factor for their intracellular target mechanism. In contrast, 9Pbw3, with two positively charged residues and Trp6 at the *C*-terminus, is a membrane targeting peptide. In order to confirm the intracellular target mechanism of 9Pbw2 and 9Pbw4, peptide distribution in bacteria should be examined further by confocal images obtained for fluorescein isothiocyanate (FITC)-labeled peptides. Currently, the therapeutic effects of these peptides are being studied in bacterially infected mice. Indeed, the peptides designed in this study may be good candidates for new antibiotic agents with potent antibacterial activity but without cytotoxicity.

Acknowledgements

This work was supported by a grant (20080401-034-017) from Biogreen 21 program, Rural Development Administration, Republic of Korea and supported by the Korea Science and Engineering Foundation(KOSEF) grant funded by the Korea government (MEST) (No. 20090076064).

References

1 Hwang J, Kang B, Kim SR, Yun E, Park K, Jeon JP, Nam S, Suh H, Hong MY, Kim I. Molecular characterization of a defensin-like peptide from larvae of a beetle, Protaetia brevitarsis. *Int. J. Ind. Entomol.* 2008; **17**: 131–135.
2 Boman HG. Peptide antibiotics and their role in innate immunity. *Annu. Rev. Immunol.* 1995; **13**: 61–92.
3 Hancock RE, Lehrer R. Cationic peptides: a new source of antibiotics. *Trends Biotechnol.* 1998; **16**: 82–88.
4 Zasloff M. Antimicrobial peptides of multicellular organisms. *Nature* 2002; **415**: 389–395.
5 Epand RM, Vogel HJ. Diversity of antimicrobial peptides and their mechanisms of action. *Biochim. Biophys. Acta* 1999; **1462**: 11–28.
6 Hancock RE, Rozek A. Role of membranes in the activities of antimicrobial cationic peptides. *FEMS Microbiol. Lett.* 2002; **206**: 143–149.
7 Otvos L Jr. Antibacterial peptides isolated from insects. *J. Pept. Sci.* 2000; **6**: 497–511.
8 Dimarcq JL, Bulet P, Hetru C, Hoffmann J. Cysteine-rich antimicrobial peptides in invertebrates. *Biopolymers* 1998; **47**: 465–477.
9 Lopez L, Morales G, Ursic R, Wolff M, Lowneberger C. Isolation and characterization of a novel insect defensin from Rhodnius prolixus, a vector of Chagas disease. *Insect Biochem. Mol. Biol.* 2003; **33**: 439–447.
10 Hultmark D. Drosophila immunity: paths and patterns. *Curr. Opin. Immunol.* 2003; **15**: 12–19.
11 Hoffmann JA. The immune response of Drosophila. *Nature* 2003; **426**: 33–38.
12 Lemaitre B. The road to toll. *Nat. Rev. Immunol.* 2004; **4**: 521–527.
13 Hoffman JA, Kafatos FC, Janeway CA, Ezekowitz RA. Phylogenic perspectives in innate immunity. *Science* 1999; **284**: 1313–1318.
14 Engstrom Y. Induction and regulation of antimicrobial peptides in Drosophila. *Dev. Comp. Immunol.* 1999; **23**: 345–358.
15 Bulet P, Hetru C, Dimarcq JL, Hoffmann D. Antimicrobial peptides in insects: structure and function. *Dev. Comp. Immunol.* 1999; **23**: 329–344.
16 Hultmark D. Immune reactions in Drosophila and other insects: a model for innate immunity. *Trends Genet.* 1993; **9**: 178–183.
17 Volkoff AN, Rocher J, d'Alencon E, Bouton M, Landais I, Quesada-Moraga E, Vey A, Fournier P, Mita K, Devauchelle G. Characterization and transcriptional profiles of three *Spodoptera frugiperdagenes* encoding cysteine-rich peptides. A new class of defensin-like genes from lepidopteran insects? *Gene* 2003; **319**: 43–53.
18 Taylor K, Barran PE, Dorin JR. Structure-activity relationships in β-defensin peptides. *Biopolymers* 2008; **90**: 1–7.
19 Hopp TP, Woods KR. Prediction of protein antigenic determinants from amino acid sequences. *Proc. Natl. Acad. Sci. USA* 1981; **78**: 3824–3828.
20 Shai Y, Bach D, Yanovsky A. Channel formation properties of synthetic pardaxin and analogues. *J. Biol. Chem.* 1990; **265**: 20202–20209.
21 Mao D, Wallace BA. Differential light scattering and absorption flattening optical effects are minimal in the circular dichroism spectra of small unilamellar vesicles. *Biochemistry* 1984; **23**: 2667–2673.
22 Zhao H, Kinnunen PK. Binding of the antimicrobial peptide temporin L to liposomes assessed by Trp fluorescence. *J. Biol. Chem.* 2002; **277**: 25170–25177.
23 Friedrich CL, Moyles D, Beveridge TJ, Hancock RE. Antibacterial action of structurally diverse cationic peptides on Gram-positive bacteria. *Antimicrob. Agents Chemother.* 2000; **44**: 2086–2092.
24 Park CB, Kim HS, Kim SC. Mechanism of action of the antimicrobial peptide buforin II: buforin II kills microorganisms by penetrating the cell membrane and inhibiting cellular functions. *Biochem. Biophys. Res. Commun.* 1998; **244**: 253–257.
25 Marion D, Wüthrich K. Application of phase sensitive two-dimensional correlated spectroscopy (COSY) for measurements of ^{1}H-^{1}H spin-spin coupling constants in proteins. *Biochem. Biophys. Res. Commun.* 1983; **113**: 967–974.
26 Derome A, Williamson M. Rapid-pulsing artifacts in double-quantum-filtered COSY. *J. Magn. Reson.* 1990; **88**: 177–185.
27 Bax A, Davis DG. Practical aspects of two-dimensional transverse NOE spectroscopy. *J. Magn. Reson.* 1985; **63**: 207–213.
28 Bax A, Davis DG. MLEV-17-based two-dimensional homonuclear magnetization transfer spectroscopy. *J. Magn. Reson.* 1985; **65**: 355–360.
29 Delaglio F, Grzesiak S, Vuister G, Zhu G, Pfeifer J, Bax A. NMRPipe: a multidimensional spectral processing system based on UNIX pipes. *J. Biomol. NMR* 1995; **6**: 277–293.
30 Goddard T, Kneller DG. *SPARKY3*, University of California: San Francisco.
31 Saido-Sakanaka H, Ishibashi J, Sagisaka A, Momotani E, Yamakawa M. Synthesis and characterization of bactericidal oligopeptides designed on the basis of an insect anti-bacterial peptide. *Biochem. J.* 1999; **338**: 29–33.
32 Yamada M, Nakamura K, Saido-Sakanaka H, Asaoka A, Yamakawa M, Yamamoto Y, Koyama Y, Hikosaka K, Shimizu A, Hirota Y. Therapeutic effect of modified oligopeptides from the beetle Allomyrina dichotoma on methicillin-resistant *Staphylococcus aureus* (MRSA) infection in mice. *J. Vet. Med. Sci.* 2005; **67**: 1005–1011.
33 Koyama Y, Motobu M, Hikosaka K, Yamada M, Nakamura K, Saido-Sakanaka H, Asaoka A, Yamakawa M, Isobe T, Shimura K, Kang CB, Hayashidani H, Nakai Y, Hirota Y. Cytotoxicity and antigenicity of antimicrobial synthesized peptides derived from the beetle Allomyrina dichotoma defensin in mice. *Int. Immunopharmacol.* 2006; **6**: 1748–1753.
34 Ghosh AK, Rukmini R, Chattopadhyay A. Modulation of tryptophan environment in membrane-bound melittin by negatively charged phospholipids: implications in membrane organization and function. *Biochemistry* 1997; **36**: 14291–14305.
35 Yu K, Kang S, Park N, Shin J, Kim Y. Relationship between the tertiary structures of mastoparan B and its analogs and their lytic activities studied by NMR spectroscopy. *J. Pept. Res.* 2000; **55**: 51–65.
36 Lee K, Shin SY, Kim K, Lim SS, Hahm KS, Kim Y. Antibiotic activity and structural analysis of the scorpion-derived antimicrobial peptide IsCT and its analogs. *Biochem. Biophys. Res. Commun.* 2004; **323**: 712–719.
37 Orioni B, Bocchinfuso G, Kim JY, Palleschi A, Grande G, Bobone S, Park Y, Kim JI, Hahm K-S, Stella L. Membrane perturbation by the antimicrobial peptide PMAP-23: a fluorescence and molecular dynamics study. *Biochim. Biophys. Acta* 2009; **1788**: 1523–1533.
38 Park CB, Yi KS, Matsuzaki K, Kim MS, Kim SC. Structure-activity analysis of buforin II, a histone H2A-derived antimicrobial peptide: the proline hinge is responsible for the cell-penetrating ability of buforin II. *Proc. Natl. Acad. Sci. USA* 2000; **97**: 8245–8250.
39 Cudic M, Otvos L Jr. Intracellular targets of antibacterial peptides. *Curr. Drug Targets* 2000; **3**: 101–106.
40 Woody RW. Contributions of tryptophan side chains to the far-ultraviolet circular dichroism of proteins. *Eur. Biophys J.* 1994; **23**: 253–262.

41 Woody RW. *Peptides, Polypeptides, and Proteins*. Wiley: New York, 1974.
42 Ladokhin AS, Selsted ME, White SH. CD spectra of indolicidin antimicrobial peptides suggest turns, not polyproline helix. *Biochemistry* 1999; **38**: 12313–12319.
43 Damberg P, Jarvet J, Graslund A. Micellar systems as solvents in peptide and protein structure determination. *Methods Enzymol.* 2001; **339**: 271–285.
44 Campagna S, Saint N, Molle G, Aumelas A. Structure and mechanism of action of the antimicrobial peptide piscidin. *Biochemistry* 2007; **46**: 1771–1778.
45 Wüthrich K. *NMR of Proteins and Nucleic Acids*. Wiley: New York, 1986.

